

Spontaneously emerging cortical representations of visual attributes

Tal Kenet*, Dmitri Bibitchkov, Misha Tsodyks, Amiram Grinvald & Amos Arieli

Department of Neurobiology, The Weizmann Institute of Science, Rehovot 76100, Israel

* Present address: Keck Center for Integrative Neurosciences, University of California San Francisco, 513 Parnassus Avenue, Box 0732, San Francisco, California 94143, USA

Spontaneous cortical activity—ongoing activity in the absence of intentional sensory input—has been studied extensively¹, using methods ranging from EEG (electroencephalography)^{2–4}, through voltage sensitive dye imaging^{5–7}, down to recordings from single neurons^{8,9}. Ongoing cortical activity has been shown to play a critical role in development^{10–14}, and must also be essential for processing sensory perception, because it modulates stimulus-evoked activity^{5,15,16}, and is correlated with behaviour¹⁷. Yet its role in the processing of external information and its relationship to internal representations of sensory attributes remains unknown. Using voltage sensitive dye imaging, we previously established a close link between ongoing activity in the visual cortex of anaesthetized cats and the spontaneous firing of a single neuron⁶. Here we report that such activity encompasses a set of dynamically switching cortical states, many of which correspond closely to orientation maps. When such an orientation state emerged spontaneously, it spanned several hypercolumns and was often followed by a state corresponding to a proximal orientation. We suggest that dynamically switching cortical states could represent the brain’s internal context, and therefore reflect or influence memory, perception and behaviour.

To determine the existence of spontaneously occurring states that correspond to cortical representations of orientations and characterize their dynamics, we chose to explore cat area 18, where most cells are selective for stimulus orientation, and therefore robust functional maps corresponding to different orientations are readily revealed. We used voltage sensitive dye imaging, which emphasizes synaptic membrane potential changes (similar to intracellular recordings from large populations of neurons^{18,19}). We recorded activity continuously in 30-s sessions (3,072 frames spaced 9.6 ms apart, covering a cortical area up to 4 × 7 mm) both in the presence and absence of stimulation (full field oriented gratings, see Methods for details). We used the evoked data to construct single-condition

and full-orientation maps, and used spatial correlation coefficients between single frames of ongoing activity and the evoked maps to evaluate similarity. Figure 1 illustrates the resemblance between a spontaneous single frame (Fig. 1b), its best correlated orientation map (Fig. 1a), and a single evoked frame (Fig. 1c). On average, the maximal correlation coefficient for evoked frames with any particular map was only 10 ± 5% higher than the maximal correlation coefficients seen for spontaneous frames (0.63 and 0.58 respectively in the example of Fig. 1). It is pertinent to note that the correlation coefficients between two maps obtained using the same stimulus, but in different recording sessions, usually ranged between 0.7 and 0.8.

To establish that such intrinsic orientation states occurred spontaneously much more frequently than expected by chance, we constructed control ‘artificial orientation maps’ (see Methods). We compared the distribution of correlation coefficients between spontaneous frames and the orientation maps (Fig. 2, red) with the corresponding distribution obtained using the control maps (Fig. 2, blue). Although both distributions were symmetrical around zero, the one computed with the real orientation maps was much wider. Specifically, whereas the maximal correlation coefficient with control patterns rarely exceeded 0.2 (less than 1% of the time), the corresponding values for the real orientation maps reached values as high as 0.6, with the mean maximal value across all hemispheres and imaging sessions being 0.5 ± 0.1. Overall, the threshold for significant correlation ($P < 0.01$) was found to range between |0.18| and |0.22| using any of the control patterns. For subsequent analysis we conservatively set the threshold for significant correlation at |0.25|. Using this threshold, we found that states corresponding to orientation maps arise spontaneously about 20% of the time. Furthermore, we found that the amplitude of the most highly correlated spontaneous states was on average only 30% lower than the amplitude of the most highly correlated evoked single frames (see Supplementary Information S11 for additional information).

To characterize the distribution of spontaneous occurrences of different orientation states, we quantified the occurrence of spontaneous frames that were significantly correlated with each of the orientation maps. The obtained distribution was biased to states corresponding to one of the cardinal orientations (0° and 90°). An example from one hemisphere is shown in Fig. 3a. Overall, the maps corresponding to the two cardinal orientations appeared 20% more often than those corresponding to the two oblique ones (45° and 135°), but this dynamical bias for different cats was highly variable, ranging from 10% to 80% (see example from three extreme cases in Fig. 3b, green). Additionally, states corresponding to oblique maps emerged with smaller correlation coefficients than cardinal ones (Fig. 3b, blue). These results indicate a strong dynamical over-

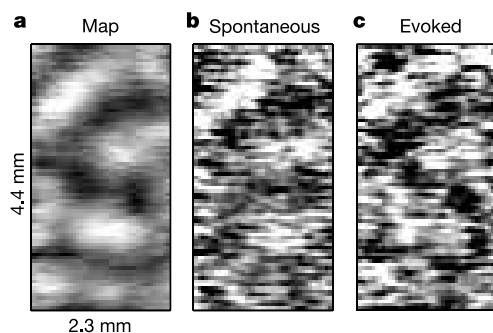


Figure 1 Comparing instantaneous patterns of spontaneous and evoked activity to the averaged functional map. **a**, The orientation map using full-field gratings of vertical orientation, obtained by averaging 165 frames (5 frames from each trial starting from 100 ms after stimulus onset, over 33 stimulus presentations). **b**, A map obtained in a single frame from a spontaneous recording session. **c**, A single frame from an evoked session using the same orientation as for the map. Amplitude was computed as described in Methods.

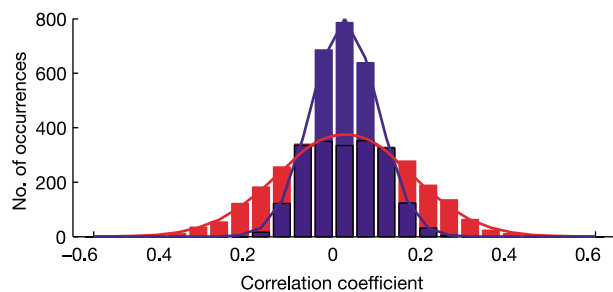


Figure 2 Spontaneously emerging orientation states. Red, example of the distribution of correlation coefficients between the horizontal map and spontaneous frames over an entire session. Blue, the same, using an inverted map. Each distribution was fitted to a gaussian to compute the significance level, |0.25| for $P < 0.01$. The distribution was similar regardless of control maps used. Actual significance values were computed from the histograms resulting from correlations with all maps. Note that although low-pass filtering the frames and maps predictably increased the value of the correlation coefficients, the number of ‘significant frames’ remained similar, as the control correlation coefficients increased proportionally.

representation of the cardinal orientations, and are in agreement with recent observations of orientation anisotropies in area 18 of the cat visual cortex^{20,21}. Interestingly, in our voltage sensitive dye maps, we did not observe any consistent over-representation of the cortical areas corresponding to the cardinal orientations. This result is in agreement with some of the previous findings²² (unlike the large bias reported for the ferret^{23,24}). This finding is intriguing, underscoring the importance of exploring both function and dynamics.

To examine the extent of the cortical area spanned by a given spontaneously emerging cortical state, we divided evoked maps into two non-overlapping regions (illustrated in Fig. 3c), and examined how each region correlated with the corresponding area in each of the instantaneous frames of ongoing activity. We found that most of the time when the significance level was crossed, the two non-overlapping regions of the state emerged either simultaneously (Fig. 3d, plus signs) or in a close temporal proximity (circles). The results are illustrated by Supplementary Information SI2 (a movie) and additional examples are shown in Supplementary Information SI3.

Finally, in order to study the intrinsic states of spontaneous population activity and their dynamics without explicitly using any stimulus-derived orientation maps, we applied a well-known Kohonen map algorithm²⁵. We began with an initial set of 40 random templates (frames) located on a closed circle, onto which the spontaneous single frames are mapped by finding the template that is closest to each frame. A Kohonen algorithm was applied to gradually update the templates so that in the end they characterize the hidden low-dimensional order in high-dimensional population activity (see Methods). A Kohonen algorithm was chosen for the analysis of the recordings because it required only spontaneous data, and did not necessitate prior assumptions about the number of hidden states. Although the templates were learned exclusively from the spontaneous data without making any use of the stimulus-evoked orientation maps, many of the 'learned templates' (after the algorithm converged) exhibited strong similarity to the orientation maps obtained from the evoked data. Figure 4A (bottom traces) depicts the templates that had highest correlation coefficients with

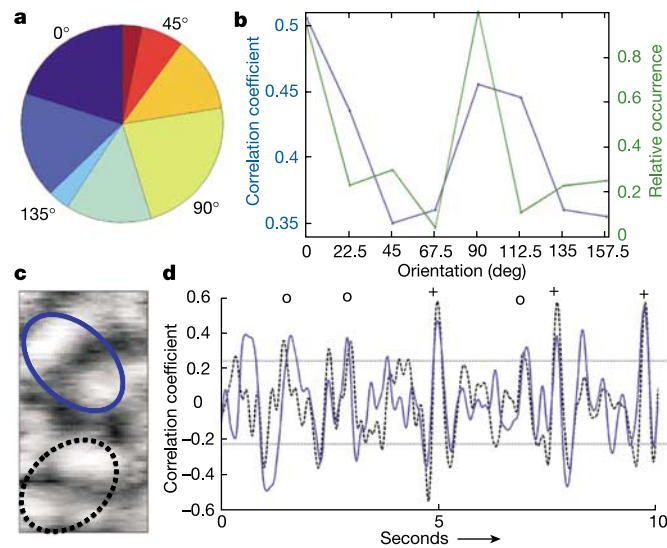


Figure 3 Dynamics of ongoing activity. **a**, Example of the distribution of occurrence of the different orientation states. **b**, The relationship between orientation and number of spontaneous occurrences of that orientation state (blue), or maximal correlation coefficient (green) (average from three hemispheres). **c**, Illustration of two non-overlapping patches on the map from Fig. 1a. **d**, Example of the time course of the correlation coefficients between each of the selected areas on an evoked map, and single frames from spontaneous activity sessions. Significance lines are plotted in accordance with Fig. 2a. Plus signs, synchronous occurrences of patches; circles, times of phase lag.

three of the orientation maps (top traces).

Because most of the final templates were good approximations to single-condition orientation maps, they could be used for estimating the orientation preference (OP) map. To this end, every template was assigned an orientation according to its position on the circle by selecting the template corresponding to horizontal orientation and adding an equal angle of 4.5° (180° divided by 40, the number of templates) to every subsequent template, and the OP of every pixel was then obtained by standard vectorial summation of the corresponding templates. The angle map calculated this way is shown in colour in Fig. 4B (right panel) together with the OP map obtained with visual stimulation (Fig. 4B, left panel). The similarity between these two maps is remarkable: the spontaneous activity alone contained most of the information about the OP maps. Figure 4Ca shows the orientation of the map that had the highest spatial correlation coefficient to each learned template. Note the systematic transitions between neighbouring orientations encountered as one moves along the set of templates. The values of the corresponding correlation coefficients are shown in Fig. 4Cb. The maximal correlation coefficients reached values as high as 0.8 for cardinal orientations, but were significantly lower for oblique orientations, in accordance with our findings of representation asymmetry.

Using the obtained templates, we analysed the dynamics of the spontaneous activity by looking at the temporal sequence of the templates onto which consecutive frames were mapped (Fig. 4Da, and movie in Supplementary Information SI4). Long epochs of smooth transitions between neighbouring templates were clearly present in the data. To check that these long epochs could not be explained merely by temporal correlations in the population activity (that is, the fact that spontaneous single frames have a finite rate of change), we performed a control analysis by generating artificial templates that had spatial structure and mutual cross-correlations similar to those of the original templates (see Methods). Using these synthetic templates indeed resulted in

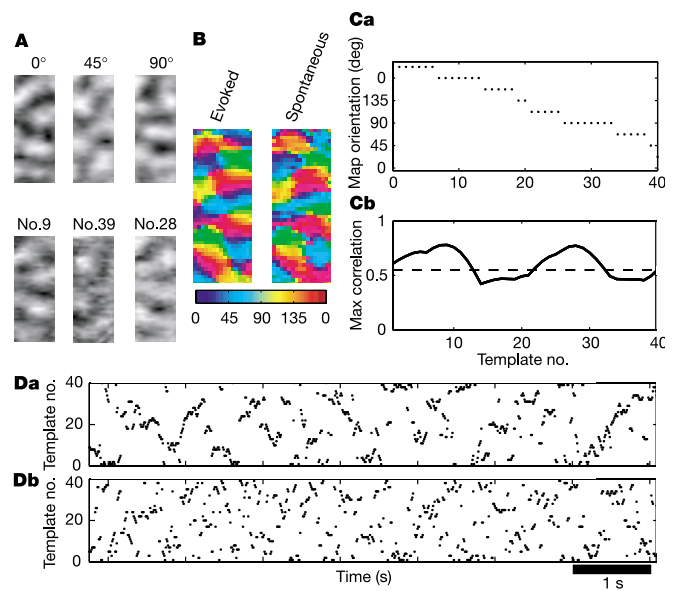


Figure 4 Spontaneous states revealed using a Kohonen algorithm. **A**, Top, three single-condition orientation maps. Bottom, three Kohonen templates best correlated with those maps. **B**, Left, evoked orientation map. Right, full orientation map computed using the 40 Kohonen templates. **Ca**, Orientation of the map that is maximally correlated to each Kohonen template. **Cb**, Correlation coefficient between each template and the corresponding orientation map. The dashed line indicates the significance level ($P < 0.01$) obtained with control synthetic templates (see Methods). **Da**, Position of a best-matching Kohonen template as a function of time. **Db**, Position of best-matching template from a set of control templates.

significantly shorter transitions (Fig. 4Db). The average transition for the experimental maps was twice as long as for the control (82 ms and 40 ms, respectively) and this difference was highly significant (t -test, $P < 10^{-16}$). The modelling of the geometry and dynamics of cortical states is further discussed in Supplementary Information SI5).

To conclude, we have shown that ongoing activity encompasses a set of dynamically switching cortical states, several of which correspond to cortical representations of orientations. The hypothesis that ongoing activity in the awake animal also contains a set of states is currently being tested. Because we do not usually perceive switching orientations while our eyes are closed, it is conceivable that states that are intrinsic to lower areas, but which are constantly interacting with incoming stimulation and feedback from higher areas²⁶, are not as persistent in duration or as spatially coherent in the awake animal as in the anaesthetized one. These findings support models of orientation maps that reflect intrinsic cortical states largely determined by intra-cortical connectivity^{27–29}, and suggest that dynamically switching cortical states could express the cortical way to prepare 'default' parameter values, which in turn reflect expectations about the sensory input. □

Methods

Imaging

We used optical imaging of voltage sensitive dyes combined with single unit recordings. The technicalities of the method are discussed extensively elsewhere^{6,7,18,30}. We used RH1691 to dye the cortex, and a high-speed camera to record the changes in the stained cortex. Data from nine hemispheres of six cats were collected and analysed (20–40 sessions per hemisphere both with and without stimulation). Each recording session lasted 30 s, and 3,072 frames 9.6 ms apart were obtained. For evoked sessions of continuous recording, over the course of the 30 s of recording, 33 stimuli of the same orientation were presented (trials). The stimuli consisted of full-field drifting gratings of high contrast lasting 200 ms, with an isoluminant 700-ms inter-stimulus interval using a grey screen. In each hemisphere, we used evoked activity to establish the basic set of states by obtaining eight single condition orientation maps at 22.5° steps. Maps in each evoked recording session were computed by averaging 165 frames; this was done by using the five frames occurring between 100 and 150 ms after stimulus onset, from each of the 33 stimuli presented over the course of a single session; $33 \times 5 = 165$). For ongoing activity recording sessions the animal's eyes were closed, and the room darkened (we found no difference when a uniform grey screen was used instead). Each recorded frame represented the instantaneous pattern of activity over a large patch of cortex (up to 4×7 mm in size; size of each pixel is $64 \times 64 \mu\text{m}$). The amplitude of each single frame was computed as the difference between the signal strength at the centres of the four most responsive patches ('white patches'), and the four least responsive patches ('black patches'). The locations of the patches were defined on the evoked maps, and for each frame we selected the map that most closely corresponded to that frame. We quantified the similarity between the patterns of any individual frame and each of the orientation maps by the correlation coefficient between the two. Note that the results in each recording session were entirely independent of stimulation history. The data was cleaned for breathing artefacts through high-pass temporal filtering above 0.6 Hz. Heart artefacts were removed by subtracting the average heart pattern for each pixel. All experiments were performed in strict accordance with institutional and NIH guidelines.

Kohonen maps

The Kohonen map algorithm was applied for a topologically ordered mapping from the space of recorded multidimensional images to a one-dimensional array of M nodes evenly distributed on a closed circle. With every node i , a template image m_i was associated. The randomly initiated templates were modified iteratively during training. Each data image $x(n)$ at a time bin n was compared with all the templates according to the euclidean distances in order to define the best-matching node (c): $c = \arg \min_i \|x - m_i\|$. The euclidean distance $\|x - m_i\|$, is a square root of a sum over all image pixels of square differences of signal intensities. The templates were then updated, such that every template was made to be slightly more similar to the current data image. The amplitude of the change for each template depends on its proximity to the best-matching node according to a neighbourhood function, $h(c - i)$: $m_i(n + 1) = m_i(n) + \alpha h(c - i)[x(n) - m_i(n)]$.

The neighbourhood function was chosen as a gaussian function of a position on the circle:

$$h(c - i) = \exp\left(-\frac{\{\min(|c - i|, M - |c - i|)\}^2}{2\sigma^2}\right)$$

For convergence it is necessary that the rate of change, α , gradually decreases during the training. We started with a value of α close to unity, and decreased it monotonically during the first training phase of 3,072 iteration steps, keeping it small (close to 0.01) afterwards. We also started with a fairly large σ , and decreased it as the proper ordering took place. The number of iterations was chosen such that each data frame is used several times (5–10). In order to construct the set of control templates, we first obtained a synthetic map by

convolution of a random image with a typical orientation preference map. The rest of the templates were formed by consequent shifts of the original synthetic map over a circular trajectory. The radius of the circle as well as the amplitudes of the shifts was chosen in such a way that resulting synthetic templates have similar cross-correlation structure to the ones obtained with the Kohonen algorithm. Significance level was calculated from a distribution of maximal correlations between orientation maps and the set of 1,000 different synthetic templates.

Received 28 April; accepted 30 September 2003; doi:10.1038/nature02078.

1. Lestienne, R. Spike timing, synchronization and information processing on the sensory side of the central nervous system. *Prog. Neurobiol.* **65**, 545–591 (2001).
2. Creutzfeldt, O. D., Watanabe, S. & Lux, H. D. Relations between EEG phenomena and potentials of single cortical cells: II. Spontaneous and convulsoid activity. *Electroenceph. Clin. Neurophysiol.* **20**, 19–37 (1966).
3. Scherrer, J. Organization of spontaneous electrical activity in the neocortex. *Prog. Brain Res.* **45**, 309–325 (1976).
4. Elul, R. The genesis of the EEG. *Int. Rev. Neurobiol.* **15**, 227–272 (1971).
5. Arieli, A., Sterkin, A., Grinvald, A. & Aertsen, A. Dynamics of ongoing activity: Explanation of the large variability in evoked cortical responses. *Science* **273**, 1868–1871 (1996).
6. Tsodyks, M., Kenet, T., Grinvald, A. & Arieli, A. Linking spontaneous activity of single cortical neurons and the underlying functional architecture. *Science* **286**, 1943–1946 (1999).
7. Arieli, A., Shoham, D., Hildesheim, R. & Grinvald, A. Coherent spatiotemporal patterns of ongoing activity revealed by real-time optical imaging coupled with single-unit recording in the cat visual-cortex. *J. Neurophysiol.* **73**, 2072–2093 (1995).
8. Noda, H. & Adey, W. R. Firing variability in cat association cortex during sleep and wakefulness. *Brain Res.* **18**, 513–526 (1970).
9. Softky, W. R. & Koch, C. The highly irregular firing of cortical cells is inconsistent with temporal integration of random EPSPs. *J. Neurosci.* **13**, 334–350 (1993).
10. Katz, L. C. & Shatz, C. J. Synaptic activity and the construction of cortical circuits. *Science* **274**, 1133–1138 (1996).
11. Thompson, I. Cortical development: A role for spontaneous activity? *Curr. Biol.* **7**, R324–R326 (1997).
12. McCormick, D. A. Developmental neuroscience — Spontaneous activity: Signal or noise? *Science* **285**, 541–543 (1999).
13. Sur, M., Angelucci, A. & Sharma, J. Rewiring cortex: The role of patterned activity in development and plasticity of neocortical circuits. *J. Neurobiol.* **41**, 33–43 (1999).
14. Chiu, C. & Weliky, M. Relationship of correlated spontaneous activity to functional ocular dominance columns in the developing visual cortex. *Neuron* **35**, 1123–1134 (2002).
15. Kiselev, M. A. & Gerstein, G. L. Trial-to-trial variability and state-dependent modulation of auditory-evoked responses in cortex. *J. Neurosci.* **19**, 10451–10460 (1999).
16. Azouz, R. & Gray, C. M. Cellular mechanisms contributing to response variability of cortical neurons *in vivo*. *J. Neurosci.* **19**, 2209–2223 (1999).
17. Adrian, E. D. & Matthews, B. H. C. The Berger rhythm: Potential changes from the occipital lobes in man. *Brain* **57**, 355–385 (1934).
18. Grinvald, A. *et al.* in *Modern Techniques in Neuroscience Research* (eds Windhorst, U. & Johansson, H.) 893–969 (Springer, Heidelberg, 1999).
19. Petersen, C. C., Grinvald, A. & Sakmann, B. Spatiotemporal dynamics of sensory responses in layer 2/3 of rat barrel cortex measured *in vivo* by voltage-sensitive dye imaging combined with whole-cell voltage recordings and neuron reconstructions. *J. Neurosci.* **23**, 1298–1309 (2003).
20. Li, B., Peterson, M. R. & Freeman, R. D. Oblique effect: A neural basis in the visual cortex. *J. Neurophysiol.* **90**, 204–217 (2003).
21. Wang, G., Ding, S. & Yunokuchi, K. Difference in the representation of cardinal and oblique contours in cat visual cortex. *Neurosci. Lett.* **338**, 77–81 (2003).
22. Bonhoeffer, T. & Grinvald, A. The layout of iso-orientation domains in area-18 of cat visual-cortex—optical imaging reveals a pinwheel-like organization. *J. Neurosci.* **13**, 4157–4180 (1993).
23. Chapman, B. & Bonhoeffer, T. Overrepresentation of horizontal and vertical orientation preferences in developing ferret area 17. *Proc. Natl Acad. Sci. USA* **95**, 2609–2614 (1998).
24. Coppola, D. M., White, L. E., Fitzpatrick, D. & Purves, D. Unequal representation of cardinal and oblique contours in ferret visual cortex. *Proc. Natl Acad. Sci. USA* **95**, 2621–2623 (1998).
25. Kohonen, T. *Self-Organizing Maps* (Springer, Berlin, 2000).
26. Fries, P., Neuenschwander, S., Engel, A. K., Goebel, R. & Singer, W. Rapid feature selective neuronal synchronization through correlated latency shifting. *Nature Neurosci.* **4**, 194–200 (2001).
27. Ben-Yishai, R., Bar-Or, R. L. & Sompolinsky, H. Theory of orientation tuning in visual-cortex. *Proc. Natl Acad. Sci. USA* **92**, 3844–3848 (1995).
28. Somers, D. C., Nelson, S. B. & Sur, M. An emergent model of orientation selectivity in cat visual cortical simple cells. *J. Neurosci.* **15**, 5448–5465 (1995).
29. Ernst, U. A., Pawelzik, K. R., Sahar-Pikielny, C. & Tsodyks, M. V. Intracortical origin of visual maps. *Nature Neurosci.* **4**, 431–436 (2001).
30. Shoham, D. *et al.* Imaging cortical dynamics at high spatial and temporal resolution with novel blue voltage-sensitive dyes. *Neuron* **24**, 791–802 (1999).

Supplementary Information accompanies the paper on www.nature.com/nature.

Acknowledgements We thank A. Aertsen, N. Tishbi, R. Malach and J. M. Herrmann for discussions and insights, R. Hildesheim for the dyes, B. Blumenfeld for his suggestion for the orientation preference map in Fig. 4B, and D. Etner and Y. Toledo for technical assistance. This work was supported by grants from the Israeli Science Foundation, Grodetsky Center and Irving B. Harris Foundation (to M.T.), the Grodetsky Center, the Korber and Israeli Science foundations and the BMBF/MOS (to A.G.) and the Minerva Foundation (to D.B.).

Competing interests statement The authors declare that they have no competing financial interests.

Correspondence and requests for materials should be addressed to T.K. (tal@phy.ucsf.edu).